

# Reconstruction of localized force distributions in cells and tissues from substrate displacements using physically-consistent regularization

We develop a method to reconstruct, from measured displacements of the underlying elastic substrate, the spatially dependent forces that cells or tissues impart on them. Since these sources of force typically arise from focal adhesions, which are localized or “compact,” and discontinuous, we solve this inverse problem using methods of optimization useful for image segmentation. In addition to the standard quadratic data mismatch terms (that defines least-squares fitting), we motivate a term in the objective function which penalizes variations in the tensor invariants of the reconstructed stress while preserving boundaries. By minimizing the objective function subject to physical constraints, we are able to efficiently reconstruct stress fields with localized structure from simulated and experimental substrate displacements. We provide a numerical method for setting up a discretized inverse problem that is solvable by standard convex optimization techniques. Our method incorporates the exact solution of the forward problem accurate to first-order finite-difference approximation in the stress tensor. For utility with newly-available high-resolution data, we motivate the use of distance-based cutoffs for data inclusion and find under loose regularity conditions the reconstruction error that results.

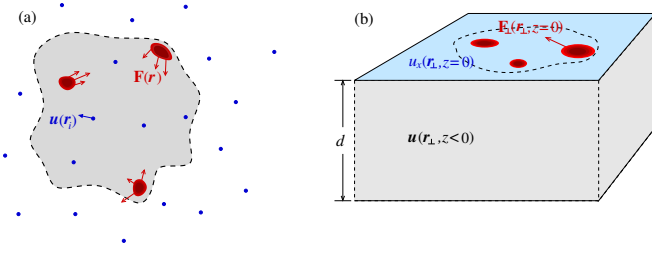


FIG. 1. A schematic of an isolated cell. (a) The boundary of the cell footprint is denoted by the dashed curve, the stress field is represented by the red regions that impart a stress  $\mathbf{F}(x, y)$  on the surface. Displacements  $\mathbf{u}(\mathbf{r}_i)$  of the elastic medium are measured at position  $\mathbf{r}_i = x_i\hat{x} + y_i\hat{y} + z_i\hat{z}$  (blue dots) that can be inside or outside the cell footprint, on the surface ( $z_i = 0$ ), or below the surface ( $z_i < 0$ ). (b). A perspective view of the elastic substrate and cellular footprint.

## INTRODUCTION

Cell motility and response to signals have hitherto almost always been studied in two-dimensional geometries in which cells are placed on a flat elastic substrate. Dynamic adhesion between the cells and the substrate are realized through *e.g.*, lamellapodia, filapodia, and dynamically reorganizing focal adhesions. Such structures are spatially localized, as shown in Fig. 1. Similarly, on larger length scales, a collection of cells can give rise to localized stress distributions. For example, the leading edge of a cell layer produces the pulling force that leads to migration in wound healing assays.

Dynamically varying force generating structures are often small and difficult to image, especially without biochemical modification such as incorporation of fluorescent dyes. Therefore, other methods for inferring their positions and magnitudes have been developed. The simplest method relies on measuring the displacement of fiducial markers, such as gold nanoparticles, embedded in the elastic substrate. The measured displacements

are an indirect probe of the force-generating structures. Any inversion method should be able to not only reconstruct the positions and magnitudes of the stress field, but should ideally be able to capture potentially sharp boundaries of the stress-generating structures.

Therefore, we develop a novel method for elastic stress source recovery using ideas developed for image segmentation. This class of methods relies on optimization that uses an  $L_1$  regularization term in the objective function. This type of regularization term is not derived from a fundamental physical law, but represents a prior knowledge that the function to be recovered is sparse in content except near edges. Nonetheless, our new objective will be constructed to obey physical constraints and symmetries.

In the next section, we review the basic linear equations of elasticity that describe the displacement field as a function of an arbitrary surface stress distribution. This model is then used to construct the data mismatch term in an objective function. We then motivate regularization and constraint terms to construct the full objective function. Finally, given simulated and experimental data, we minimize our objective function using a modified split-Bregman algorithm and reconstruct the given stress fields. Our method provides good reconstruction of localized structures that exhibit desirable qualities such as the suppression of Gibbs ringing phenomenon at the boundaries of the stress structures.

## ELASTIC MODEL

In this section, we explicitly describe the elastic green’s function associated with a point force applied to the surface of a semi-infinite half-space, as shown in Fig. 1(b). The domain of the elastic medium is  $\mathcal{D} = \{(x, y, z) | x, y \in \mathbb{R}, z \leq 0\}$ . We assume that the elastic medium is infinite in depth ( $d \rightarrow \infty$ ) and lateral extent.

The Green's function

$$\mathbf{G}^0 = \begin{bmatrix} G_{xx}^0(x, y, z) & G_{xy}^0(x, y, z) & G_{xz}^0(x, y, z) \\ G_{yx}^0(x, y, z) & G_{yy}^0(x, y, z) & G_{yz}^0(x, y, z) \\ G_{zx}^0(x, y, z) & G_{zy}^0(x, y, z) & G_{zz}^0(x, y, z) \end{bmatrix} \quad (1)$$

for linear isotropic elasticity theory in the half-space is given by its components

$$G_{ss}^0(x, y, z) = \frac{1 + \nu}{2\pi E} \left[ \frac{2(1 - \nu)R_{\perp} - z}{R_{\perp}(R_{\perp} - z)} + \frac{[2R_{\perp}(\nu R_{\perp} - z) + z^2]s^2}{R_{\perp}^3(R_{\perp} - z)^2} \right], \quad (2)$$

$$G_{zz}^0(x, y, z) = \frac{1 + \nu}{2\pi E} \left( \frac{2(1 - \nu)}{R_{\perp}} + \frac{z^2}{R_{\perp}^3} \right), \quad (3)$$

$$G_{xy}^0(x, y, z) = G_{yx}^0 = \frac{1 + \nu}{2\pi E} \frac{[2R_{\perp}(\nu R_{\perp} - z) + z^2]xy}{R_{\perp}^3(R_{\perp} - z)^2}, \quad (4)$$

$$G_{sz, zs}^0(x, y, z) = \frac{1 + \nu}{2\pi E} \left( \frac{sz}{R_{\perp}^3} \pm \frac{(1 - 2\nu)s}{R_{\perp}(R_{\perp} - z)} \right), \quad (5)$$

where  $s = x, y$  the equation with  $\pm$  corresponds to  $G_{sz}^0$  and  $G_{zs}^0$ , respectively, and  $R_{\perp} \equiv \sqrt{x^2 + y^2}$ . The Young's modulus and Poisson ratio of the elastic substrate are denoted by  $E$  and  $\nu$ , respectively. The displacement of a material point at  $(x, y, z \leq 0)$  in the medium due to a stress distribution  $\mathbf{F}$  is simply the convolution  $\mathbf{u}(\mathbf{r}) \equiv [u_x \ u_y \ u_z]^T = \mathbf{G}^0 * \mathbf{F}$ .

For our specific problem, we shall specialize the forces to surface stresses  $\sigma_{x,y}$  that act on the plane perpendicular to the  $\hat{z}$  axis. We define the in-plane stress distribution, at depth  $z$ , as  $\boldsymbol{\sigma}(x, y, z) = \sigma_{xz}(x, y, z)\hat{x} + \sigma_{yz}(x, y, z)\hat{y}$ . The resulting surface-level displacement fields become

$$u_x(x, y) = \int_{\Omega} dx' dy' G_{xx}(x - x', y - y') \sigma_{xz}(x', y') + \int_{\Omega} dx' dy' G_{xy}(x - x', y - y') \sigma_{yz}(x', y') \quad (6)$$

$$u_y(x, y) = \int_{\Omega} dx' dy' G_{yx}(x - x', y - y') \sigma_{xz}(x', y') + \int_{\Omega} dx' dy' G_{yy}(x - x', y - y') \sigma_{yz}(x', y'), \quad (7)$$

where

$$G_{\cdot, \cdot}(x, y) = G_{\cdot, \cdot}^0(x, y, z = 0), \quad (8)$$

and by abuse of notation,

$$\sigma_{xz}(x, y) = \sigma_{xz}(x, y, z = 0) \quad \sigma_{yz}(x, y) = \sigma_{yz}(x, y, z = 0). \quad (9)$$

Note that tangential stresses can lead to displacement data in the normal direction.

### SETUP OF INVERSE PROBLEM

Here, we develop an objective function for which the minimizing solution provides a good approximation to the underlying stress field, while preserving discontinuities. The first component is simply a quadratic data mismatch term defined by the sum over the displacements measured at the  $N$  measurement positions at  $\mathbf{r}_i$ :

$$\Phi_{\text{data}}[\boldsymbol{\sigma}] = \sum_i^N |\mathbf{u}^{\text{data}}(\mathbf{r}_i) - \mathbf{u}(\mathbf{r}_i)|^2. \quad (10)$$

Since  $\mathbf{u}^{\text{data}}(\mathbf{r}_i)$  is given, and  $\mathbf{u}(\mathbf{r}_i)$ , is given by Eqs. 6 and 7, this contribution to the objective function is a functional over the surface-stress function  $\boldsymbol{\sigma}(\mathbf{r}_{\perp})$ . For simplicity, we will assume that the data points are sampled over an uniform grid with coordinates given  $\{(x_j, y_k) : j \in \{1, 2, \dots, J\}, k \in \{1, 2, \dots, K\}\}$ .

In Eqs 6 and 7, we have restricted the domain of integration to the extent of the cell,  $\Omega$ , to emphasize that  $\boldsymbol{\sigma}$  has compact support. As a consequence of compact support, for a fixed, discretized approximation of  $\sigma_{xz}, \sigma_{yz}$ , the displacements can be obtained exactly by solving an equivalent system of linear equations of finite dimension.

Here we explicitly define this system of linear equations given a piecewise-affine approximation of the stress field. Let us consider the first-order approximation of  $\sigma_{xz}$  and  $\sigma_{yz}$  using central finite differences, for  $x \in [x_j - \delta x/2, x_j + \delta x/2] \cap y \in [y_j - \delta y/2, y_j + \delta y/2]$ ,

$$\begin{aligned} \sigma_{xz}(x, y) &= \sigma_{xz}(x_i, y_j) \\ &+ (x - x_i) \frac{\sigma_{xz}(x_{i+1}, y_j) - \sigma_{xz}(x_{i-1}, y_j)}{2\delta x} \\ &+ (y - y_j) \frac{\sigma_{xz}(x_i, y_{j+1}) - \sigma_{xz}(x_i, y_{j-1})}{2\delta y} \\ &+ \mathcal{O}(\delta x)^2 + \mathcal{O}(\delta y)^2, \end{aligned} \quad (11)$$

where  $i, j$  denotes a tuple of grid coordinates. In effect, we are performing sub-pixel interpolation of the stress where the stress is fully-determined by its values at the grid vertices.

Now we may rewrite Eq. 6, for instance, to solve for the displacement at a location  $(x_n, y_m)$ , by decomposing the integral into a sum of integrals over grid cells

$$\begin{aligned}
u_x(x_n, y_m) = & \sum_{(x_j, y_k) \in \Omega} \left\{ \left[ \sigma_{xz}(x_j, y_k) - x_j \left( \frac{\sigma_{xz}(x_{j+1}, y_k) - \sigma_{xz}(x_{j-1}, y_k)}{2\delta x} \right) - y_k \left( \frac{\sigma_{xz}(x_j, y_{k+1}) - \sigma_{xz}(x_j, y_{k-1})}{2\delta y} \right) \right] \langle G_{xx} \rangle^{nmjk} \right. \\
& + \left[ \frac{\sigma_{xz}(x_{j+1}, y_k) - \sigma_{xz}(x_{j-1}, y_k)}{2\delta x} \right] \langle xG_{xx} \rangle^{nmjk} + \left[ \frac{\sigma_{xz}(x_j, y_{k+1}) - \sigma_{xz}(x_j, y_{k-1})}{2\delta y} \right] \langle yG_{xx} \rangle^{nmjk} \\
& + \left[ \sigma_{yz}(x_j, y_k) - x_j \left( \frac{\sigma_{yz}(x_{j+1}, y_k) - \sigma_{yz}(x_{j-1}, y_k)}{2\delta x} \right) - y_k \left( \frac{\sigma_{yz}(x_j, y_{k+1}) - \sigma_{yz}(x_j, y_{k-1})}{2\delta y} \right) \right] \langle G_{xy} \rangle^{nmjk} \\
& \left. + \left[ \frac{\sigma_{yz}(x_{j+1}, y_k) - \sigma_{yz}(x_{j-1}, y_k)}{2\delta x} \right] \int_{y_k - \delta y/2}^{y_k + \delta y/2} \langle xG_{xy} \rangle^{nmjk} + \left[ \frac{\sigma_{yz}(x_j, y_{k+1}) - \sigma_{yz}(x_j, y_{k-1})}{2\delta y} \right] \langle yG_{xy} \rangle^{nmjk} \right\}, \quad (12)
\end{aligned}$$

where

$$\langle G_{st} \rangle^{nmjk} = \int_{y_k - \delta y/2}^{y_k + \delta y/2} \int_{x_j - \delta x/2}^{x_j + \delta x/2} G_{st}(x_n - x', y_m - y') dx' dy' \quad (13)$$

$$\langle f(x, y) G_{st} \rangle^{nmjk} = \int_{y_k - \delta y/2}^{y_k + \delta y/2} \int_{x_j - \delta x/2}^{x_j + \delta x/2} f(x', y') G_{st}(x_n - x', y_m - y') dx' dy', \quad (14)$$

except that at the edges where we use one-sided differences so that we are only differentiating within  $\Omega$ . Explicit closed-form expressions for the integrals represented in Eqs. 13 and 14 are given in the Supplemental Materials. A similar expression can be found for solving for  $u_y$  (not shown).

Regrouping terms, we can now define the linear system of equations for solving for  $u_x$  at all grid points simultaneously,

$$u_x^{nm} = X^{nmjk} \sigma_{xz}(x_j, y_k) + Y^{nmjk} \sigma_{yz}(x_j, y_k), \quad (15)$$

where summation is implied over each index tuple  $(j, k)$ , and the coefficient matrices are defined as

$$\begin{aligned}
X^{nmjk} = & \langle G_{xx} \rangle^{nmjk} - \langle G_{xx} \rangle^{n,m,j-1,k} \frac{x_{j-1}}{2\delta x} \\
& + \langle G_{xx} \rangle^{n,m,j+1,k} \frac{x_{j+1}}{2\delta x} - \langle G_{xx} \rangle^{n,m,j,k-1} \frac{y_{k-1}}{2\delta y} \\
& + \langle G_{xx} \rangle^{n,m,j,k+1} \frac{y_{k+1}}{2\delta y} - \frac{\langle xG_{xx} \rangle^{n,m,j-1,k}}{2\delta x} \\
& + \frac{\langle xG_{xx} \rangle^{n,m,j+1,k}}{2\delta x} - \frac{\langle yG_{xx} \rangle^{n,m,j,k-1}}{2\delta y} \\
& + \frac{\langle yG_{xx} \rangle^{n,m,j,k+1}}{2\delta y} \quad (16)
\end{aligned}$$

$$\begin{aligned}
Y^{n,m,j,k} = & \langle G_{xy} \rangle^{nmjk} - \langle G_{xy} \rangle^{n,m,j-1,k} \frac{x_{j-1}}{2\delta x} \\
& + \langle G_{xy} \rangle^{n,m,j+1,k} \frac{x_{j+1}}{2\delta x} - \langle G_{xy} \rangle^{n,m,j,k-1} \frac{y_{k-1}}{2\delta y} \\
& + \langle G_{xy} \rangle^{n,m,j,k+1} \frac{y_{k+1}}{2\delta y} - \frac{\langle xG_{xy} \rangle^{n,m,j-1,k}}{2\delta x} \\
& + \frac{\langle xG_{xy} \rangle^{n,m,j+1,k}}{2\delta x} - \frac{\langle yG_{xy} \rangle^{n,m,j,k-1}}{2\delta y} \\
& + \frac{\langle yG_{xy} \rangle^{n,m,j,k+1}}{2\delta y}. \quad (17)
\end{aligned}$$

From the equation-counting perspective, the system of equations is exactly determined given that one has at least as many measurement points as grid cells in the resolution that one wishes to reconstruct the stress field, provided that one is able to measure displacements in both principle directions. However, in line experiments this is not the case. Furthermore, even if one is able to measure both displacements, the problem may still be highly ill-conditioned since measurements are taken in the presence of noise at a finite precision. To resolve these issues, we introduce the concept of physically consistent regularization as applied to this problem.

### Physical regularization

So far, the construction of the surface stress, even at the finite resolution where measurements are available, is ill-conditioned. We regularize this problem, by forcing the reconstruction to obey some physically-relevant characteristics of the surface stress. First, since we are assuming inertial effects are negligible, we require that the net force is zero, or that

$$\int_{\Omega} \sigma_{xz}(x, y) dx dy = \int_{\Omega} \sigma_{yz}(x, y) dx dy = 0. \quad (18)$$

Likewise, we require that there is no net torque, or that

$$\int_{\Omega} \sigma_{yz}(x, y) x dx dy = \int_{\Omega} \sigma_{xz}(x, y) y dx dy. \quad (19)$$

Finally, we would like to impose regularity on the reconstructed fields while preserving first rotational invariance and second sharp interfaces. To this end we employ a variant of a penalty used often in image processing applications, where we wish to penalize the  $L_1$  norm of the variation in the fields, or the total variation. To do this in such a manner that is consistent with the philosophy that rotation of the data should not affect the result, we penalize the total variation norm of the invariants of the stress tensor. In the case of two-dimensional tensors, of which the surface stress is an example, the tensor invariants are the trace

$$\text{Tr}(\boldsymbol{\sigma}) = \sigma_{xx} + \sigma_{yy} \quad (20)$$

and the determinant

$$\text{Det}(\boldsymbol{\sigma}) = \sigma_{xx}\sigma_{yy} - \sigma_{xy}^2. \quad (21)$$

Any regularization penalty imposed on the reconstruction problem must be a functional of these invariants in order to maintain rotational invariance, relative to the choice of observation frame, of the reconstructed stress tensor.

### Sparsity-Enforcing priors

For this manuscript, we will use the trace, but we note that it may also be natural to use the logarithm of the determinant, in analogy to the log-likelihood arising in multivariate linear regression problems of unknown variance. We now write the convex regularization functional,  $\Phi = \|\sigma_{xx} + \sigma_{yy}\|_{TV}$  the total variation of the trace of the tensor,

$$\Phi = \int_{\Omega} |\nabla(\sigma_{xx}(x', y') + \sigma_{yy}(x', y'))| dx' dy'. \quad (22)$$

The corresponding penalized optimization problem

$$\boldsymbol{\sigma}^* | \lambda = \arg \min_{\boldsymbol{\sigma}} \{ \Phi_{\text{data}}[\boldsymbol{\sigma}] + \lambda \Phi[\boldsymbol{\sigma}] \}, \quad (23)$$

subject to the constraints mentioned above, where  $\lambda > 0$  is a tunable parameter. This problem is linear and is solvable within standard optimization routines. In our implementation, we use a second-order quadratic cone solver.

### Cut-off

To reduce the size of the system of equations described in Eqs. 15–17, we note that the Green's function falls off at a rate of  $r^{-1}$ . However, when combined with the zero-force constraint, the relationship between the displacements and the support of the stress field falls off at the much quicker rate of  $r^{-2}$  under a set of reasonable assumptions.

**Lemma 1.** *Let  $\Omega = \text{supp}(\boldsymbol{\sigma}) \subset \mathbb{R}^2$  be compact, and assume that  $\boldsymbol{\sigma} \in L^1(\Omega)$ . For a fixed  $\mathbf{x} \notin \Omega$ , denote  $D(\mathbf{x}) = \inf\{\|\mathbf{x} - \mathbf{y}\| : \mathbf{y} \in \Omega\}$ . Then, if  $D(\mathbf{x}) \geq R > 0$ , then*

$$|u_x(\mathbf{x})| \leq \frac{C_x \|\boldsymbol{\sigma}\|_1}{R^2} \quad (24)$$

and

$$|u_y(\mathbf{x})| \leq \frac{C_y \|\boldsymbol{\sigma}\|_1}{R^2} \quad (25)$$

for some constants  $C_x, C_y$ .

*Proof.* □

The decay of the influence of stress on the system provides justification for setting distance-based cut-offs specification of the linear system. The effect of the cut-off is to limit the left-hand side of Eq. 15 to only locations within some maximal distance  $R$  from the outline of the cell. The error in the solution of the inverse problem is dependent on the precision of the observations, the physical constants that describe the medium, and the maximum magnitude of the stress.

**Theorem 2.** *Proof.* □

## RESULTS

We implemented our regularized inversion method in Python version 3.5, where optimization is performed using the `cvxpy` package.

### Comparison of norms

## SUMMARY AND CONCLUSIONS

### Integrals

$$\begin{aligned} & \int_{y_k - \delta y/2}^{y_k + \delta y/2} \int_{x_j - \delta x/2}^{x_j + \delta x/2} G_{xx}(x - x', y - y') dx' dy' \\ &= \int_{\Delta y_k^-}^{\Delta y_k^+} \int_{\Delta x_j^-}^{\Delta x_j^+} G_{xx}(u, v) du dv \\ &= \frac{\nu + 1}{2\pi E} \int_{\Delta y_k^-}^{\Delta y_k^+} \left[ 2 \log \left( \sqrt{(\Delta x_j^+)^2 + v^2} \right) - \frac{2\nu \Delta x_j^+}{\sqrt{(\Delta x_j^+)^2 + v^2}} \right] dv \\ &\quad - \frac{\nu + 1}{2\pi E} \int_{\Delta y_k^-}^{\Delta y_k^+} \left[ 2 \log \left( \sqrt{(\Delta x_j^-)^2 + v^2} \right) - \frac{2\nu \Delta x_j^-}{\sqrt{(\Delta x_j^-)^2 + v^2}} \right] dv \\ &= f_{xx}(\Delta x_j^+, \Delta y_k^+) - f_{xx}(\Delta x_j^+, \Delta y_k^-) \\ &\quad - f_{xx}(\Delta x_j^-, \Delta y_k^+) + f_{xx}(\Delta x_j^-, \Delta y_k^-) \end{aligned} \quad (26)$$

where

$$f_{xx}(x, y) = \frac{\nu + 1}{\pi E} \left[ x(1 - \nu) \log \left( \sqrt{x^2 + y^2} + y \right) + y \log \left( \sqrt{x^2 + y^2} + x \right) - y \right]. \quad (27)$$